DALTON

Reactions of transition-metal oxo complexes with $B(C_6F_5)_3$: crystal structures of $[V\{OB(C_6F_5)_3\}(acac)_2]$, $[Ti\{OB(C_6F_5)_3\}(acac)_2]$ and *cis*-$[MoO\{OB(C_6F_5)_3\}(acac)_2]$ (acac = acetylacetonate)

Jane R. Galsworthy,[a] **Malcolm L. H. Green,**[a] **Matthias Müller**[b] **and Keith Prout**[b]

[a] *Inorganic Chemistry Laboratory, South Parks Road, Oxford OX1 3QR, UK*
[b] *Chemical Crystallography Laboratory, 9 Parks Road, Oxford OX1 3PD, UK*

The transition-metal oxo complexes $[VO(acac)_2]$, $[\{TiO(acac)_2\}_2]$ and *cis*-$[MoO_2(acac)_2]$ (acac = $C_5H_7O_2$) reacted with the strong Lewis acid $B(C_6F_5)_3$ to give the structurally characterized complexes $[V\{OB(C_6F_5)_3\}(acac)_2]$, $[Ti\{OB(C_6F_5)_3\}(acac)_2]$ and *cis*-$[MoO\{OB(C_6F_5)_3\}(acac)_2]$. The M=O–B moiety is essentially linear.

Transition-metal oxo complexes play significant roles in both hetero- and homo-geneous catalysis, chemical and biochemical oxidation processes.[1,2] The oxo group may act as a bridge between the catalyst and cocatalyst.[3] In certain catalytic reactions the activity of the oxo metal complex is increased by addition of a Lewis-acid cocatalyst whilst in others it is essential for the production of a catalytically active species and interaction between the Lewis acid and the oxo function is implicated. Osborn and co-workers[3,4] synthesized both the complex $[WO(CH_2Bu^t)_3Br]$ and the Lewis-acid adduct $[W(OAlBr_3)(CH_2Bu^t)_3Br]$ which has been crystallographically characterized. The latter compound is a moderately active alkene-metathesis catalyst whilst the former is completely inactive. The difference in reactivity has been tentatively ascribed to a greater electrophilicity of the metal centre in the Lewis acid–base adduct complex.

Recently we have been exploring the varied chemistry of the readily available, crystalline Lewis acid $B(C_6F_5)_3$.[5] Here we describe studies into its reactivity with transition-metal oxo complexes.

Results and Discussion

Treatment of each of the transition-metal oxo complexes $[VO(acac)_2]$, $[\{TiO(acac)_2\}_2]$ and *cis*-$[MoO_2(acac)_2]$ (acac = $C_5H_7O_2$) with 1 equivalent of $B(C_6F_5)_3$ in toluene under ambient conditions yields the oxo metal–Lewis acid adducts as dark green $[V\{OB(C_6F_5)_3\}(acac)_2]$ **1**, yellow $[Ti\{OB(C_6F_5)_3\}(acac)_2]$ **2** and red-orange *cis*-$[MoO\{OB(C_6F_5)_3\}(acac)_2]$ **3**, respectively. The compounds **1**–**3** are more soluble than the starting metal compounds and can be crystallized from toluene solution. The crystals are air stable but the vanadyl complex **1** contains a toluene molecule of crystallization which is gradually lost once the filtrate is removed.

Complexes **1**–**3** have been characterized by crystal structure determination and by IR and ^1H, ^{11}B, ^{13}C and ^{19}F NMR spectroscopies (Table 1). An expected upfield shift of the ^{11}B NMR spectroscopic resonance of $B(C_6F_5)_3$ (δ 51) to around δ 0 is observed upon formation of the dative M=O–B bond. The latter signal is typical of a four-co-ordinate boron species. No measure of the strength of the M=O–B interaction could be made using IR spectroscopy as the fluorinated aryl rings absorb strongly in the region 1100–900 cm^{-1} preventing assignment of the characteristic M=O stretch. We would expect that co-ordination of the oxo metal group to the boron centre would reduce the IR frequency of the M=O stretch by approximately 50 cm^{-1}. For example a related complex, $[V(OBPh_3)(C_{22}H_{22}N_4)]$, exhibits a strong peak at 919 cm^{-1}, 46 cm^{-1} lower than that observed for the parent vanadyl complex.[6]

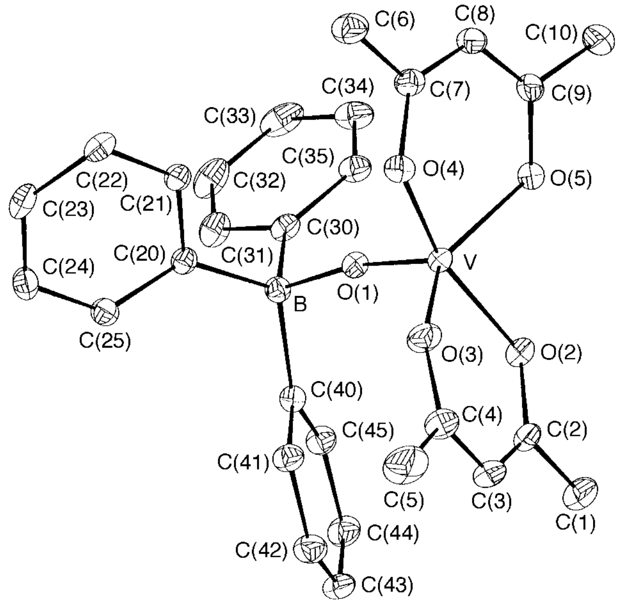

Fig. 1 Structure of $[V\{OB(C_6F_5)_3\}(acac)_2]$ **1**. Fluorine atoms are omitted for clarity

The molecular structure of compound **1** is shown in Fig. 1. The vanadium centre has a square-based pyramidal geometry with the four oxygen atoms of the acac ligands occupying the basal sites. The V=O distance of 1.648(1) Å is significantly longer than that of the parent compound (1.56 Å)[7] reflecting a reduction in bond order on complexation of the boron Lewis acid to the oxo group. The B–O distance of 1.527(2) Å is typical of a boron–oxygen single bond and a virtually linear V–O–B arrangement [168.9(1)°] is found. These observations are in accord with *ab initio* calculations of the electronic structure of $[VO(acac)_2]$ which describe the V=O bond as possessing partial triple-bond character.[8a] A similar elongation of the V=O bond was observed for $[VO(C_{22}H_{22}N_4)]$ (1.601 Å) on formation of the complex $[V(OBPh_3)(C_{22}H_{22}N_4)]$ (1.665 Å).[6]

Compound **2** is the first example of a crystallographically characterized titanyl–Lewis acid adduct. The square-based pyramidal structure adopted by **2** (Fig. 2) is remarkably similar to that of **1** although the B–O bond length of 1.496(3) Å is shorter reflecting perhaps a stronger dative interaction with the boron centre. The Ti–O bond distance [1.698(2) Å] is slightly longer than previously reported for formal Ti=O double bonds (1.61–1.68 Å);[8b] there are relatively few examples of such a bond. In general, the earlier transition-metal oxo complexes display a preference for bridging metal–oxo linkages as exhibited by the

Table 1 Analytical and spectroscopic data for compounds **1**–**3**

Complex[a]	Spectroscopic data[b]
1 $[V\{OB(C_6F_5)_3\}(acac)_2]\cdot C_6H_5Me$ C, 43.6 (43.2); H, 1.9 (1.8); B, 1.3 (1.4)[c] Mass: *m/z* 512 $[B(C_6F_5)_3]$, 265 $[VO(acac)_2]$	IR: 3100–2800w, 1646vs, 1518vs, 1468vs, 1380vs, 1342vs, 1288vs, 1185m, 1101vs, 1031s, 985vs, 855m, 817m, 794m, 734m, 682s, 612m, 576m, 504s, 475m ^{1}H:[d] 7.19 (5 H, m, C_6H_5Me), 3.5 (vbr, f.w.h.h. 300 Hz, $C_5H_7O_2$), 2.34 (3 H, m, C_6H_5Me) ^{13}C:[d] 148.2 (m, C_6F_5), 138.1 (m, C_6F_5), 128.7 (d, C_6H_5Me), 125.4, 24.2 (s, CH_3), 21.3 (s, C_6H_5Me) ^{11}B:[d] −1.9 (br) ^{19}F:[d] 35 (vbr), 7.9 (s), 0.7 (s)
2 $[Ti\{OB(C_6F_5)_3\}(acac)_2]$ C, 43.7 (43.4); H, 1.6 (1.8); B, 1.3 (1.4) Mass: *m/z* 512 $[B(C_6F_5)_3]$, 263 $[TiO(acac)_2]$	IR: 2950–2850w, 1645m, 1536vs, 1516vs, 1469vs, 1391m, 1371m, 1362m, 1294m, 1280m, 1093s, 1031vs, 989vs, 978vs, 939s, 811m, 797m, 771m, 764m, 677m, 511m, 475m ^{1}H: 5.01 (1 H, s, CH), 1.55 (6 H, s, CH_3) ^{13}C: 195.0 (s, CO), 149.9 (dt, *J* 239.0, 8.8, C_6F_5), 139.9 (dt, *J* 247.5, 14.6, C_6F_5), 137.4 (ddd, *J* 245.1, 18.7, 8.9, C_6F_5), 106.7 (s, CH) ^{11}B: 1.5 (br) ^{19}F: 34.2 (dd, *J* 24.9, 8.9, C_6F_5), 7.5 (t, *J* 21.1, C_6F_5), 1.4 (td, *J* 24.4, 5.2, C_6F_5)
3 *cis*-$[MoO\{OB(C_6F_5)_3\}(acac)_2]$ C, 40.1 (40.1); H, 1.7 (1.7); B, 1.4 (1.3) Mass: *m/z* 512 $[B(C_6F_5)_3]$, 326 $[MoO_2(acac)_2]$	IR: 3000–2850w, 1645s, 1603s, 1584s, 1514vs, 1468vs, 1381m, 1357m, 1272s, 1185m, 1101s, 1026m, 978s, 937m, 910s, 808m, 791m, 772m, 747w, 675m ^{1}H: 4.93 (1 H, s, CH), 4.82 (1 H, s, CH), 1.55 (3 H, s, Me), 1.43 (3 H, s, Me), 1.37 (1 H, s, CH), 1.34 (3 H, s, Me) ^{13}C: 198.8 (s, CO), 195.9 (s, CO), 187.2 (s, CO), 183.2 (s, CO), 148.6 (d, *J* 250.1, C_6F_5), 140.5 (d, C_6F_5), 137.6 (d, *J* 270.8, C_6F_5), 106.9 (d, CH), 105.5 (s, CH), 27.7 (s, CH_3), 26.7 (s, CH_3), 24.4 (s, CH_3), 23.2 (s, CH_3) ^{11}B: 4.7 (br) ^{19}F: 33.9 (dd, *J* 24.5, 7.5, C_6F_5), 9.0 (t, *J* 20.7, C_6F_5), 2.2 (dt, *J* 24.9, 8.9, C_6F_5)

[a] Analytical data given as found (calculated) in %. [b] IR data (cm^{-1}) determined as KBr discs; NMR (C_6D_6, 298 K), unless otherwise stated, given as chemical shift (δ) [relative intensity, multiplicity (*J* in Hz), assignment]; f.w.h.h. = full width at half height. [c] The solvent of crystallization may be removed by subjecting crystals to high vacuum for extended periods of time. [d] In CD_2Cl_2.

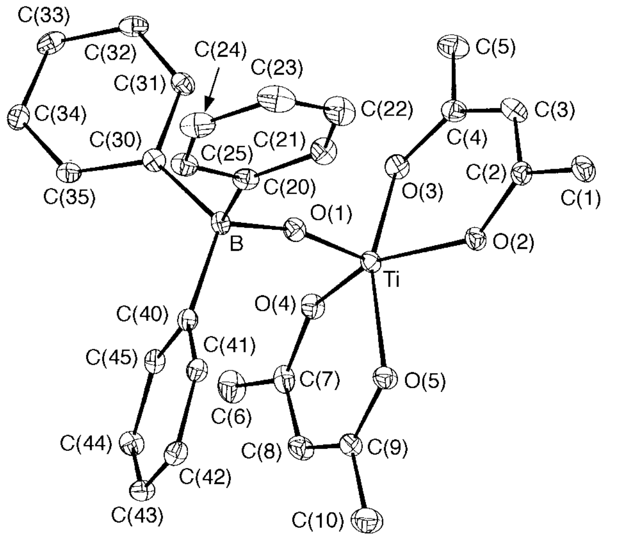

Fig. 2 Structure of $[Ti\{OB(C_6F_5)_3\}(acac)_2]$ **2**. Fluorine atoms are omitted for clarity

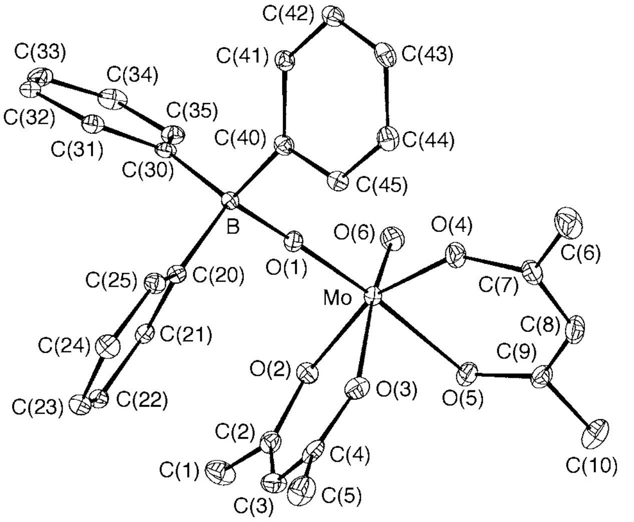

Fig. 3 Structure of *cis*-$[MoO\{OB(C_6F_5)_3\}(acac)_2]$ **3**. Fluorine atoms are omitted for clarity

parent complex $[\{TiO(acac)_2\}_2]$, a binuclear titanium species containing two bridging Ti–O–Ti units.[9] In the crystalline state the Ti=O–B unit present in compound **2** exhibits only a slight deviation from linearity [165.8(2)°]. Only one related oxo metal–Lewis acid adduct, $[Zr(\eta\text{-}C_5Me_5)_2\{OB(C_6F_5)_3\}]$, formed from the reaction of $[NEt_3H][(C_6F_5)_3BOH]$ with $[Zr(\eta\text{-}C_5Me_5)_2Me_2]$, has been structurally characterized in Group 4 chemistry.[10] It contains a $(C_6F_5)_3BO$ moiety co-ordinated to zirconium and the B–O bond length is 1.487(3) Å. One of the C_6F_5 rings is oriented so that its *o*-fluorine forms a Zr–F–C bridge which is maintained in solution as determined by low-temperature (−88 °C) ^{19}F NMR spectroscopy.

The crystal structure of complex **3** (Fig. 3) reveals that the *cis* arrangement of the two Mo=O units is maintained upon co-ordination of $B(C_6F_5)_3$ to one of the Mo=O moieties. The B–O bond length [1.521(3) Å] is typical of those found within this family of compounds and again the Mo=O–B grouping is virtually linear [171.2(1)°]. The presence of one Mo=O–$B(C_6F_5)_3$ moiety and one terminal Mo=O unit within **3** allows us to assess the electron-withdrawing abilities of the boron Lewis acid. A significant lengthening, of approximately 0.1 Å, is observed for the Mo=O bond upon co-ordination; Mo–O(1) 1.772(2), Mo–O(6) 1.682(2) Å. Examination of the structure suggests that the metal centre is too crowded to bind a second $B(C_6F_5)_3$ molecule at the second available oxo metal site. This is borne out experimentally by the reaction of $[MoO_2(acac)_2]$ with 2 equivalents of $B(C_6F_5)_3$ which results only in the formation of complex **3**. Compound **3** is the first example of an oxo molybdenum–Lewis acid adduct. There is no NMR spectroscopic evidence to suggest that the boron moiety undergoes any fluxional behaviour at room temperature; the ^{1}H NMR spectrum of **3** exhibits four distinct resonances assigned to the methyl groups of the acac ligands indicating that the two (acac) ligands are inequivalent on the NMR time-scale. Two closely related tungsten complexes have been structurally characterised, $[WO_2L(OBPh_3)]$ and $[(WO_3L)_2BPh_2][BPh_4]$ (L = 1,4,7-triazacyclononane).[11] Table 2 provides a comparison of various M–O–L bond angles, where L = Lewis acid, for related compounds. The crystal structure of $[V(OBPh_3)(C_{22}H_{22}N_4)]$ has

Table 2 Comparison of M=O–L bond angles, L = Lewis acid, for oxo metal complexes

Compound	M–O–L/°
1 [V{OB(C_6F_5)$_3$}(acac)$_2$]	168.9(1)
2 [Ti{OB(C_6F_5)$_3$}(acac)$_2$]	165.8(1)
3 [MoO{OB(C_6F_5)$_3$}(acac)$_2$]	171.2(1)
[Zr(C_5Me_5)$_2${OB(C_6F_5)$_3$}][10]	151.2(3)
[V(OSnPh$_2$Cl$_2$)(salen)]·H$_2$O[12,a]	172.1
[V(OSnPh$_2$Cl$_2$)(mosalen)]·H$_2$O[12,b]	163.8
[W(OAlBr$_3$)(CH$_2$Bu^t)$_3$Br][3]	172(1)
[WO$_2$L(OBPh$_3$)][11,c]	154.2(10)

[a] H$_2$salen = *N*,*N'*-bis(salicylidene)ethane-1,2-diamine. [b] mosalen = 3,3′-dimethoxy analogue of salen. [c] L = 1,4,7-Triazacyclononane.

Table 3 Selected bond distances (Å) and angles (°) for compound **1**

V–O(1)	1.648(1)	V–O(4)	1.943(1)
V–O(2)	1.945(1)	V–O(5)	1.907(1)
V–O(3)	1.909(1)	O(1)–B	1.527(2)
O(1)–V–O(2)	100.45(6)	O(1)–V–O(5)	111.53(6)
O(1)–V–O(3)	112.97(7)	B–O(1)–V	168.9(1)
O(1)–V–O(4)	102.58(6)		

been reported but no details of the V–O–L bond angle were given.

In order to probe the strength of the M=O–B interaction the reaction of complex **1** with pyridine was investigated. Detailed studies have been made into the reactions of [VO(acac)$_2$] with pyridine and its derivatives.[12] In most cases the pyridine species occupies the sixth co-ordination site at the metal centre to form an octahedral complex. The reaction of a green C_6D_6 solution of **1** with 1 equivalent of pyridine resulted in the immediate formation of an orange solution followed by a second, gradual change to turquoise; after about 12 h no traces of the orange species were visible. The first colour change, green to orange, was accompanied by a shift in the ^{11}B NMR spectroscopic signal from δ −1.9 to −4.0. No ^{1}H NMR spectroscopic signals were visible, apart from those assigned to toluene which derives from the solvent incorporated into the crystal lattice of compound **1**. This is consistent with all ligands being bound in close proximity to the paramagnetic vanadium(IV) centre. The final blue solution was identified as containing [VO(acac)$_2$] and C_5H_5N·B(C_6F_5)$_3$ by *in situ* ^{1}H and ^{11}B NMR spectroscopic data. Repetition of the reaction on a larger scale enabled the isolation and identification of the products by comparison of their spectroscopic properties with those of authentic samples. It is tempting to suggest that pyridine initially attacks the metal centre to yield the orange kinetic product, proposed to be [V{OB(C_6F_5)$_3$}(py)(acac)$_2$], and then migrates to the boron atom, displacing the V=O–B interaction, to form C_5H_5N·B(C_6F_5)$_3$ (Scheme 1).

To assess the basicity of the oxo metal grouping towards oxophilic boron Lewis acids we also investigated reactions with BPh$_3$ and B(C_6F_5)$_2$Cl. The complexes [VO(acac)$_2$], [{TiO(acac)$_2$}$_2$] and *cis*-[MoO$_2$(acac)$_2$] all failed to react with BPh$_3$; ^{11}B NMR spectroscopic data revealed that the sole boron-containing species present in each reaction mixture was unchanged BPh$_3$. This underlines the much weaker Lewis acidity of BPh$_3$ relative to its perfluorinated analogue.[13]

Treatment of [VO(acac)$_2$] with B(C_6F_5)$_2$Cl yielded a dark green compound with ^{11}B NMR spectrum (δ 5.0) similar to that obtained for compound **1** (δ −1.9) and thus in keeping with the molecular formula [V{OB(C_6F_5)$_2$Cl}(acac)$_2$]. However, attempts to crystallize the product, by cooling a concentrated toluene solution of [V{OB(C_6F_5)$_2$Cl}(acac)$_2$], produced crystals of [VO(acac)$_2$] and B(C_6F_5)$_2$Cl although the only species present in the supernatant liquid was [V{OB(C_6F_5)$_2$Cl}(acac)$_2$]. This indicates only that the combined lattice energies of the reagents, [VO(acac)$_2$] and B(C_6F_5)$_2$Cl, are greater than that of the product, [V{OB(C_6F_5)$_2$Cl}(acac)$_2$], and does not allow us to infer anything about the relative oxophilicities of B(C_6F_5)$_3$ and B(C_6F_5)$_2$Cl.

In conclusion we have demonstrated that the oxo group in transition-metal oxo complexes is sufficiently nucleophilic to form a dative interaction with B(C_6F_5)$_3$. The reactions are facilitated by the strong electrophilicity of B(C_6F_5)$_3$ as demonstrated by the inability of the weaker Lewis acid, BPh$_3$, to yield analogous adducts.[14] The M=O–B(C_6F_5)$_3$ interaction is reasonably strong and stable to air although it may be displaced by strong bases such as pyridine.

Table 4 Selected bond distances (Å) and angles (°) for compound **2**

Ti–O(1)	1.698(2)	Ti–O(4)	1.955(2)
Ti–O(2)	1.940(2)	Ti–O(5)	1.954(2)
Ti–O(3)	1.948(2)	O(1)–B	1.496(3)
O(1)–Ti–O(2)	107.31(9)	O(1)–Ti–O(5)	102.58(9)
O(1)–Ti–O(3)	105.51(9)	B–O(1)–Ti	165.8(2)
O(1)–Ti–O(4)	105.06(8)		

Table 5 Selected bond distances (Å) and angles (°) for compound **3**

Mo–O(1)	1.772(2)	Mo–O(5)	2.093(2)
Mo–O(2)	1.965(2)	Mo–O(6)	1.682(2)
Mo–O(3)	2.163(2)	O(1)–B	1.521(3)
Mo–O(4)	1.956(2)		
O(1)–Mo–O(2)	99.30(7)	O(1)–Mo–O(5)	167.44(7)
O(1)–Mo–O(3)	87.65(7)	O(1)–Mo–O(6)	102.48(8)
O(1)–Mo–O(4)	93.35(8)	B–O(1)–Mo	171.2(1)

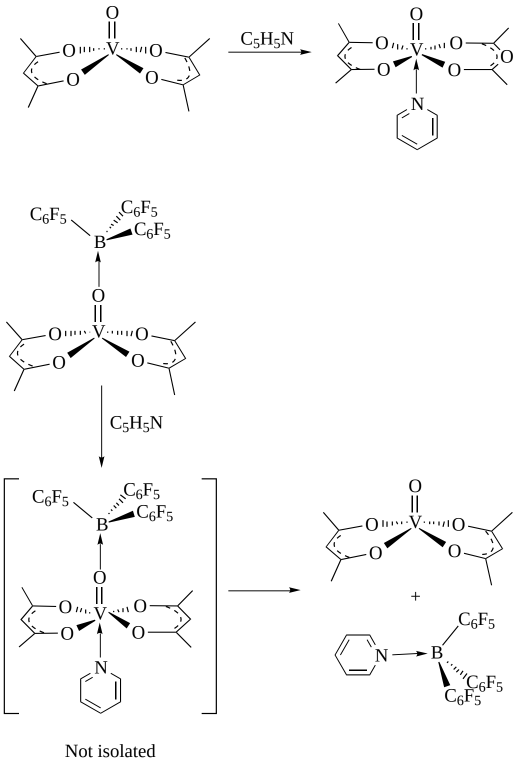

Scheme 1 A comparison of the reaction of [VO(acac)$_2$] with C_5H_5N and the proposed pathway for the reaction of [V{OB(C_6F_5)$_3$}(acac)$_2$] **1** with C_5H_5N

Experimental

Fourier-transform ^{1}H and ^{11}B NMR spectra were recorded on a Bruker WM 300 spectrometer at 300 and 96 MHz respectively, ^{13}C NMR spectra on a Bruker WM 300 at 75.5 MHz or

AM 500 spectrometer at 125 MHz and ^{19}F NMR spectra on a Bruker AM 500 spectrometer at 147 MHz: ^{1}H and ^{13}C shifts are reported with respect to δ 0 for $SiMe_4$, ^{11}B with respect to δ 0 for $BF_3{\cdot}OEt_2$ and ^{19}F with respect to δ 0 for CHF_3; all downfield shifts are positive. Infrared spectra were recorded on either a Mattson 'Polaris' Fourier-transform, Perkin-Elmer FT 1710 or Perkin-Elmer 457 grating spectrometers. Mass spectra were obtained by Dr. Ballantine at the SERC facility at the University of Swansea (for FAB) on a Varian E 109 instrument. Microanalyses were obtained from the microanalytical department of this department.

All reactions were carried out under nitrogen using standard Schlenk techniques. Solvents were dried over suitable reagents and freshly distilled under N_2 before use. The compounds $[VO(acac)_2]$, $[\{TiO(acac)_2\}_2]$ and *cis*-$[MoO_2(acac)_2]$ were used as received (Aldrich), BPh_3 was obtained from Aldrich and recrystallized prior to use and $B(C_6F_5)_3$[15] and $B(C_6F_5)_2Cl$[16] were prepared as previously described.

Preparations

$[V\{OB(C_6F_5)_3\}(acac)_2]$ 1. The compound $[VO(acac)_2]$ (0.530 g, 2 mmol) was partially dissolved in toluene (20 cm^3) and a toluene solution (20 cm^3) of $B(C_6F_5)_3$ (1.024 g, 2 mmol) added. The mixture was stirred for 2 h during which a dark green solution formed. After removal of solvent *in vacuo* the residue was washed with pentane and the desired product then extracted into toluene. This solution was concentrated and cooled to −20 °C resulting in the formation of large block-shaped green crystals of **1** in virtually quantitative yield.

$[Ti\{OB(C_6F_5)_3\}(acac)_2]$ 2. The compound $[\{TiO(acac)_2\}_2]$ (0.263 g, 1 mmol) was partially dissolved in toluene (20 cm^3) and a toluene solution (20 cm^3) of $B(C_6F_5)_3$ (1.024 g, 2 mmol) added. The mixture was stirred for 4 h during which a yellow solution formed. After removal of solvent *in vacuo* the residue was washed with pentane and the desired product then extracted into toluene. This solution was concentrated and cooled to −20 °C resulting in the formation of small yellow crystals of **2**. Yield: 0.57 g, 74%.

***cis*-$[MoO\{OB(C_6F_5)_3\}(acac)_2]$ 3.** The complex $[MoO_2(acac)_2]$ (0.652 g, 2 mmol) was partially dissolved in toluene (20 cm^3) and a toluene solution (20 cm^3) of $B(C_6F_5)_3$ (1.024 g, 2 mmol) added. The mixture was stirred for 2 h during which time a deep orange solution formed. After removal of solvent *in vacuo* the residue was washed with pentane and the desired product then extracted into toluene. Removal of the solvent *in vacuo* yielded analytically pure compound **3**. Alternatively orange-red crystals of **3** could be grown by concentrating the toluene solution and layering it with pentane. Yield: 1.46 g, 87.1%.

Reaction of $[VO(acac)_2]$ with $B(C_6F_5)_2Cl$

The complex $[VO(acac)_2]$ (0.265 g, 1 mmol) was partially dissolved in toluene (20 cm^3) and a toluene solution (20 cm^3) of $B(C_6F_5)_2Cl$ (0.381g, 1 mmol) added. The mixture was stirred for 2 h during which time a dark green solution formed. After removal of solvent *in vacuo* the residue was washed with pentane and a dark green solution extracted into toluene and then pumped to dryness to yield $[V\{OB(C_6F_5)_2Cl\}(acac)_2]$ **4**. NMR (C_6D_6, 298 K): ^{1}H (300 MHz), δ 4.7 [1 H, s(br), CH] and 1.57 [6 H, s(br), CH_3]; ^{11}B, δ −5.0. Attempts to crystallize **4** from a concentrated toluene solution at −20 °C resulted in the formation of crystals of $[VO(acac)_2]$ and $B(C_6F_5)_2Cl$.

Reaction of $[V\{OB(C_6F_5)_3\}(acac)_2]$ 1 with pyridine

The complex $[V\{OB(C_6F_5)_3\}(acac)_2]$ (0.155 g, 0.2 mmol) was dissolved in toluene (10 cm^3) and C_5H_5N (0.2 mmol) in toluene (10 cm^3) added. Immediately the green solution turned orange and after stirring for 15 min the solvent was removed. On standing (12 h) the oily orange solid became turquoise. Extraction with toluene allowed the isolation of $C_5H_5N{\cdot}B(C_6F_5)_3$. NMR ($C_6D_6$, 298 K): ^{1}H, δ 9.74 (2 H), 8.59 (1 H) and 8.22 (2 H); ^{11}B, δ −4.3. The residual turquoise solid was identified as $[VO(acac)_2]$ by ^{1}H NMR spectroscopy.

Reactions with BPh_3

The complex $[VO(acac)_2]$ (0.530 g, 2 mmol) was partially dissolved in toluene (20 cm^3) and a toluene solution (20 cm^3) of BPh_3 (0.484 g, 2 mmol) added. The mixture was stirred for 48 h at ambient temperature. No reaction was observed.

Similarly, $[\{TiO(acac)_2\}_2]$ (0.526 g, 2 mmol), pale yellow suspension stirred for 24 h, and *cis*-$[MoO_2(acac)_2]$ (0.326 g, 1 mmol), mixture stirred for 48 h at ambient temperature, gave no reaction.

Crystallography

Crystals of compounds **2** and **3** were grown from toluene solutions at 253 K and then dried *in vacuo*; those of **1** were grown from toluene solution and then stored in the mother liquid to prevent the loss of included toluene from the crystals. In each case a crystal was immersed in highly viscous perfluoropolyether to exclude oxygen and prevent solvent loss. It was then mounted on a glass fibre and plunged in a cold (150 K) nitrogen stream.

Crystal data. Compound **1**, $C_{28}H_{14}BF_{15}O_5V{\cdot}C_7H_8$, $M = 869.29$, monoclinic, space group $C2/c$, $a = 20.108(3)$, $b = 11.053(4)$, $c = 31.448(8)$ Å, $\beta = 90.480(2)°$, $U = 6989.2$ Å^3, $Z = 8$, $D_c = 1.652$ g cm^{-3}, $\mu = 3.927$ cm^{-1}, transparent green prism, crystal dimensions 0.2 × 0.3 × 0.4 mm. Compound **2**, $C_{28}H_{14}BF_{15}O_5Ti$, $M = 774.1$, monoclinic, space group $P2_1/n$, $a = 10.034(1)$, $b = 26.779(2)$, $c = 11.095(1)$ Å, $\beta = 96.97(2)°$, $U = 2959.0$ Å^3, $Z = 4$, $D_c = 1.74$ g cm^{-3}, $\mu = 4.14$ cm^{-1}, yellow block, crystal dimensions 0.14 × 0.14 × 0.22 mm. Compound **3**, $C_{28}H_{14}BF_{15}MoO_6$, $M = 838.13$, monoclinic, space group $P2_1/c$, $a = 13.735(1)$, $b = 17.991(1)$, $c = 12.490(1)$ Å, $\beta = 106.367(2)°$, $U = 2961.3$ Å^3, $Z = 4$, $D_c = 1.88$ g cm^{-3}, $\mu = 5.651$ cm^{-1}, orange block, crystal dimensions 0.25 × 0.25 × 0.16 mm.

Data collection and processing. The data for compounds **1** and **3** were collected at 150 K on an Enraf-Nonius DIP2020 image-plate diffractometer with graphite-monochromated Mo-Kα radiation ($\lambda = 0.710\,69$ Å). An Oxford Cryosystems CRYOSTREAM cooling system was used. For compound **1** 32 687 reflections were measured ($1 < \theta < 26°$, $-24 \leqslant h \leqslant 24$, $-13 \leqslant k \leqslant 13$, $-39 \leqslant l \leqslant 39$), 6788 unique of which 6253 had $I > 2\sigma(I)$. For compound **3** 35 260 reflections were measured ($1 < \theta < 26°$, $-15 \leqslant h \leqslant 15$, $-22 \leqslant k \leqslant 22$, $-17 \leqslant l \leqslant 17$), 6169 unique of which 5047 had $I > 4\sigma(I)$. The images were processed with the DENZO and SCALEPACK programs.[17] The data for compound **2** were collected at 150 K on an Enraf-Nonius FAST diffractometer with graphite-monochromated Mo-Kα radiation ($\lambda = 0.710\,69$ Å). 11 582 Reflections were measured ($1 < \theta < 25°$, $-11 \leqslant h \leqslant 11$, $-29 \leqslant k \leqslant 29$, $-12 \leqslant l \leqslant 12$), 4216 unique of which 3329 had $I > \sigma(I)$. Corrections for Lorentz-polarization effects were performed but not for absorption and extinction.

Structure solution and refinement. The crystal structures were solved by direct methods and refined by the full-matrix least-squares method. Compound **1** crystallized with toluene in a 1 : 1 ratio. Two distinct toluene molecules were found: one lying with its molecular two-fold axis along a crystallographic two-fold axis, the other being disordered at a crystallographic inversion centre with a translation of about 0.8 Å along its molecular two-fold axis. All non-hydrogen atoms of **1** and of the ordered toluene molecule were refined with anisotropic displacement parameters. The carbon atoms of the disordered toluene molecule were treated isotropically using the same isotropic displacement parameter for all seven carbon atoms. All hydrogen atoms could be located in Fourier-difference maps. The two non-methyl hydrogen atoms were refined isotropically. The hydrogen atoms of the toluene methyl group were not placed. All other hydrogen atoms were added geometrically and included in the final refinement with fixed positional and thermal parameters. 506 Refined parameters and 6253 observations resulted in a ratio observations : refined parameters of 12.4 : 1. A Chebyshev weighting scheme[18] with parameters 1.90, 1.12, 1.32, 0.195 and 0.326 was applied. Refinement on F converged to $R = 0.045$, $R' = 0.047$ and goodness of fit = 1.10. A final Fourier-difference synthesis showed minimum and maximum residual electron densities of -0.59 and 0.64 e Å^{-3}.

For compound **2** all non-hydrogen atoms were refined in anisotropic and the two non-methyl hydrogen atoms in isotropic approximation. All hydrogen atoms could be located in Fourier-difference maps. The methyl hydrogen atoms were placed geometrically and included in the final refinement with fixed positional and thermal parameters. A correction for anomalous scattering was applied and refinement completed using a Chebyshev weighting scheme[18] with parameters 12.0, -4.53 and 10.0. 459 Refined parameters and 3321 observations resulted in a ratio observations : refined parameters of 7.2 : 1. Refinement on F converged to $R = 0.040$, $R' = 0.043$ and goodness of fit = 1.11. A final Fourier-difference synthesis showed minimum and maximum residual electron densities of -0.52 and 0.47 e Å^{-3}.

For compound **3** the non-hydrogen and the two non-methyl hydrogen atoms were refined as for **2**. 5047 Observations for 468 refined parameters resulted in an observations : refined parameters ratio of 10.8 : 1. Subsequent treatment was as for **2** (Chebyshev weighting scheme[18] parameters 2.00, 0.0481 and 1.75). Refinement on F converged to $R = 0.040$, $R' = 0.037$ and goodness of fit = 1.15. A final Fourier-difference synthesis showed minimum and maximum residual electron densities of -0.88 and 0.74 e Å^{-3}. All crystallographic calculations were carried out using the CRYSTALS program package.[19] Neutral atom scattering factors were taken from ref. 20.

Atomic coordinates, thermal parameters, and bond lengths and angles have been deposited at the Cambridge Crystallographic Data Centre (CCDC). See Instructions for Authors, *J. Chem. Soc., Dalton Trans.*, 1997, Issue 1. Any request to the CCDC for this material should quote the full literature citation and the reference number 186/414.

Acknowledgements

We thank the University of Oxford for a Violette and Samuel Glasstone Fellowship (to J. R. G.), the Deutsche Forschung Gemeinschaft (M. M.) and the EPSRC for support of this work.

References

1 A. K. Rappe and W. A. Goddard III, *J. Am. Chem. Soc.*, 1982, **104**, 448.
2 R. A. Sheldon and J. K. Kochi, *Metal-catalysed Oxidations of Organic Compounds*, Academic Press, New York, 1981.
3 J. Fischer, J. Kress, J. A. Osborn, L. Ricard and M. Wesolek, *Polyhedron*, 1987, **6**, 1839.
4 J. Kress, M. Wesolek, J.-P. Le Ny and J. A. Osborn, *J. Chem. Soc., Chem. Commun.*, 1982, 1039.
5 M. L. H. Green, J. Haggitt and C. P. Mehnert, *J. Chem. Soc., Chem. Commun.*, 1985, 1853.
6 C.-H. Yang, J. A. Ladd and V. L. Goedken, *J. Coord. Chem.*, 1988, **18**, 317.
7 R. P. Dodge, D. H. Templeton and A. Zalkin, *J. Chem. Phys.*, 1965, **43**, 3111.
8 (*a*) S. Di Bella, G. Lanza, A. Gulino and I. Fragala, *Inorg. Chem.*, 1996, **35**, 3885; (*b*) A. Bodner, P. Jeske, T. Weyhermuller, K. Wieghardt, E. Dubler, H. Scmalle and B. Nuber, *Inorg. Chem.*, 1992, **31**, 3737.
9 G. D. Smith, C. N. Caughlin and J. A. Campbell, *Inorg. Chem.*, 1972, **11**, 2989.
10 A. R. Siedle, R. A. Newmark, W. M. Lamanna and J. C. Huffman, *Organometallics*, 1993, **12**, 1491.
11 P. Schreiber, K. Wieghardt, B. Nuber and J. Weiss, *Z. Naturforsch, Teil B*, 1990, **45**, 619.
12 B. Cashin, D. Cunningham, J. F. Gallagher and P. McArdle, *Polyhedron*, 1989, **8**, 1753.
13 M. J. Macazaga, J. A. Garcia-Vazquez, R. M. Medina and J. R. Masaguer, *Transition Met. Chem.* (*Weinheim, Ger.*), 1983, **8**, 215.
14 J. M. Miller and M. Onyszchuk, *Can. J. Chem.*, 1964, **42**, 1518.
15 A. G. Massey and A. J. Park, *J. Organomet. Chem.*, 1964, **2**, 245.
16 R. D. Chambers and T. Chivers, *J. Chem. Soc.*, 1965, 3933.
17 D. Gewirth, *The HKL Manual*, written with the co-operation of the program authors, Z. Otwinowski and W. Minor, Yale University, 1995.
18 E. Prince, *Mathematical Techniques in Crystallography and Material Sciences*, Springer, New York, 1982.
19 D. J. Watkins, C. K. Prout, J. R. Carruthers and P. W. Betteridge, CRYSTALS Issue 10, Chemical Crystallography Laboratory, University of Oxford, 1996.
20 *International Tables for Crystallography*, Kluwer, Dordrecht, 1992, vol. C.

Received 2nd *December* 1996; *Paper* 6/08140A